# Change of deformation mechanisms in ultrafine grained Mg-Zn-Zr-Ca alloy

IOP Conf. Series: Materials Science and Engineering **194** (2017) 012016 doi:10.1088/1757-899X/194/1/012016

# Change of deformation mechanisms in ultrafine grained Mg-Zn-Zr-Ca alloy

**Ruixiao Zheng[1], Tilak Bhattacharjee[1,2], Akinobu Shibata[1,2], Taisuke Sasaki[3], Kazuhiro Hono[3], Nobuhiro Tsuji[1,2]**

[1] Department of Materials Science and Engineering, Kyoto University, Yoshida Honmachi, Sakyo-ku, Kyoto 606-8501, Japan
[2] Elements Strategy Initiative for Structural Materials (ESISM), Kyoto University
[3] National Institute for Materials Science, 1-2-1 Sengen, Tsukuba 305-0047, Japan

E-mail: zheng.ruixiao.7m@kyoto-u.ac.jp

**Abstract**. In this study, a fully recrystallized ultrafine grained (UFG) Mg-Zn-Zr-Ca alloy was successfully fabricated by a process including high pressure torsion (HPT) and subsequent rapid annealing. Room temperature tensile test revealed that the UFG Mg alloy with a mean grain size of 0.98 μm exhibited simultaneously enhanced strength and ductility compared to those of the coarse grained counterpart (grain size 57 μm). Observation of deformation microstructures revealed that {10-12} deformation twinning and basal slip were the dominant deformation mechanisms in the coarse grained specimen, while deformation twinning was significantly inhibited but non-basal slip systems seemed activated in the UFG specimen. The reason for the enhanced mechanical properties in the UFG specimen was discussed based on the change of deformation mechanisms observed.

## 1. Introduction

In recent years, Magnesium (Mg) alloys have attracted extensive attention due to their low density and high specific strength. They are expected to be applied in transportation and aerospace industries as structural components, achieving significant weight reduction [1-3]. However, their hexagonal close-packed (HCP) crystal structure provides only a limited number of independent slip systems, resulting in relatively low tensile ductility as well as poor formability at room temperature [4]. Therefore, up to date, most Mg alloys are still used in their cast state, which cannot have taken their full advantage.

Grain refinement is considered as one of the most promising ways for optimizing strength without sacrificing ductility [5]. To achieving grain refinement, many strategies have been developed. Among them, severe plastic deformation (SPD) processes, such as equal channel angular pressing (ECAP), accumulative roll bonding (ARB) and high pressure torsion (HPT), have already been proven as effective approaches for realizing significant grain refinement [6]. A survey of available scientific literatures has demonstrated that for Mg alloys, ECAP is mostly applied at relatively high temperatures to avoid cracking [7]. However, due to the effect of dynamic recovery and recrystallization at elevated temperatures, minimum grain sizes obtained in the ECAP-processed Mg alloys are usually around several micrometers.

In contrast, high hydrostatic pressure is applied to disc-shaped specimens during torsion deformation in HPT, so that undesirable cracking can be avoided even at room temperature [8-10].

Very recently, Meng *et al*. [9] carried out HPT deformation on Mg-3.4Zn (at.%) alloy at ambient temperature and found that equiaxed grains with an average diameter of 140 nm could be obtained after HPT by 20 revolutions. However, due to the high density of retained lattice defects (such as dislocations), the HPT-processed NC/UFG Mg alloys did not show good ductility. Thus, their mechanical properties were characterized only by using simple hardness test. In order to overcome the above deficiency of HPT-processed Mg alloys, a process including room temperature HPT and subsequent annealing treatment is proposed in the present study. A Mg-Zn-Zr-Ca (ZKX600) alloy is selected for realizing optimal nanostructures. Microstructure observation and mechanical property test reveal that fully recrystallized UFG ZKX600 Mg alloy with simultaneously enhanced strength and ductility is successfully obtained. The deformation microstructures of several representative specimens are observed after tensile deformation to specified strains. The change of deformation mechanisms are discussed based on the deformation microstructures observed.

## 2. Experimental Procedures

The as-received ZKX600 Mg alloy ingot with a composition of Mg-6.2%Zn-0.5%Zr-0.2%Ca (mass%) was firstly homogenized at 350 $^{o}$C for 48 h followed by a solid solution treatment (ST) at 400 $^{o}$C for 1 h using a box-type resistance furnace. Disc-shaped samples with diameter of 10 mm and thickness of 0.80 mm sliced from the ingot were provided for HPT. HPT was conducted at room temperature under a compressive pressure of 6 GPa at a rotation speed of 0.2 rpm. The total rotation angle applied was 360$^{o}$. After HPT, the specimen was provided for an annealing treatment at 400 $^{o}$C for 1 min, using a salt bath furnace.

The areas at a radial distance of 3.0 mm from the center on transverse sections involving the rotation axis of the HPT-processed discs were observed by transmission electron microscopy (TEM) using JEOL 2010 operated at 200 kV. The areas at a distance of 3.0 mm from the center on sections perpendicular to the rotation axis of the annealed discs were characterized by field emission scanning electron microscopy (FE-SEM) using JSM 7100F equipped with an electron backscattering diffraction (EBSD) system. The grain size was measured by linear interception method on the obtained EBSD maps.

Mechanical properties of the samples were characterized by uniaxial tensile test. Small-sized tensile specimens with a gauge length of 2 mm and a cross section of 1 mm × 0.5 mm were cut from the discs at a radial distance of 2.5 mm from the center, so that the tensile direction is perpendicular to the radial direction. Tensile tests were carried out at a quasi-static strain rate of $8.3\times10^{-4}$ $s^{-1}$, with a direct measurement of the displacement of the gauge section using a CCD video camera extensometer.

## 3. Results and Discussion

Figure 1 shows (a) an EBSD inverse pole figure (IPF) map indicating crystallographic orientations parallel to the normal direction of the as-ST disc specimen and (b) a bright field TEM micrograph of the 360° HPT processed specimen. The EBSD-IPF map (Figure 1 (a)) exhibits that the as-ST specimen shows a coarse grained structure with a mean grain size of about 57 μm and does not have strong crystallographic texture. Nearly equiaxed nanocrystlline structure was obtained by 360$^{o}$ HPT rotations, as shown in Figure 1 (b). The mean grain size is about 100 nm, which is significantly finer than that of pure Mg (grain size ~1 μm) subjected to the HPT process under the similar rotation angles [11]. The result indicates that the alloying elements in the present alloy play important roles in reducing the grain size obtained by SPD. In addition, the ring-like selected area electron diffraction (SAED) pattern inserted in Figure 1 (b) indicates that the nano-grains have various orientations.

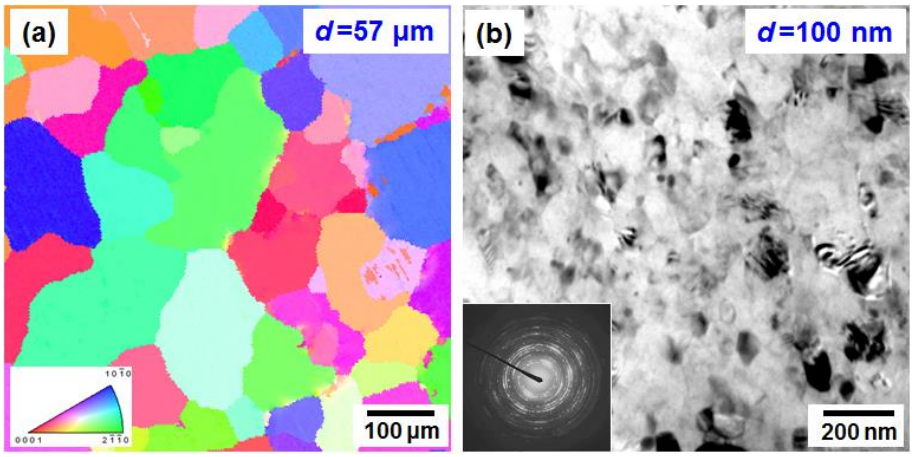


**Figure 1**. (a) EBSD-IPF map of the as-ST specimen showing coarse grained structure with a mean grain size of about 57 μm. (b) Bright field TEM image of the 360° HPT processed specimen showing nearly equiaxed nanocrystalline structure with a mean grain size of about 100 nm.

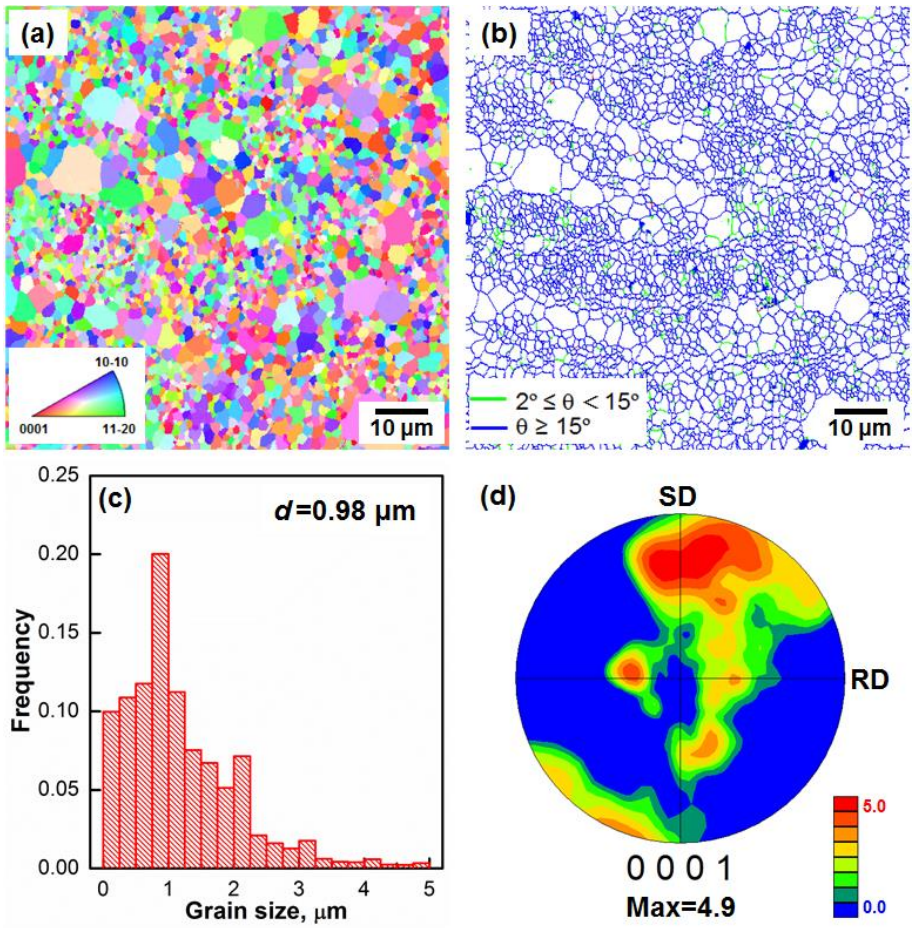


**Figure 2**. EBSD results of the specimen HPT processed by 360° rotation and then annealed at 400 °C for 1 min. (a) IPF map and (b) corresponding GB map showing fully recrystallized UFG structure. (c) Statistical histogram showing the grain size distribution. (d) (0001) pole figure showing weak texture. SD and RD represent shear direction and radius direction, respectively.

Figure 2 shows EBSD results of the specimen HPT processed by 360° and then annealed at 400 °C for 1 min. The colors in the IPF map (a) indicate crystallographic orientations parallel to the normal direction of the HPT disc. The blue and green lines in the grain boundary (GB) map (b) correspond to high angle grain boundaries (HAGBs) having misorientations larger than 15° and low angle grain boundaries (LAGBs) with misorientations between 2° and 15°, respectively. After the rapid annealing at 400 °C for 1 min, a fully recrystallized UFG structure with a mean grain size of 0.98 μm (Fig. 2 (c)) was successfully obtained. In addition, the peak intensity was low and the peak intensity regions located far from the center in the (0001) pole figure (Fig. 2 (d)), indicating that the basal texture usually observed in wrought Mg alloys is not seen in the present annealed specimen.

For understanding the mechanical properties of the alloy processed under different conditions, several representative specimens were subjected to the tensile test and obtained nominal stress-strain curves are presented in Figure 3 (a). For the as-ST specimen with a coarse mean grain size of 57 μm, the yield strength, ultimate tensile strength, uniform elongation and total elongation were 107 MPa, 256 MPa, 13.9% and 16.5%, respectively. After the HPT process by 360° rotation, the yield strength greatly increased to 311 MPa, which was almost three times higher than that of the as-ST specimen. However, the tensile ductility (total elongation) dropped to 1.2%. After annealing at 400 °C for 1 min, the yield strength and ultimate tensile strength of the specimen with the mean grain size of 0.98 μm (Fig.2) were 213 MPa and 317 MPa, respectively. The uniform elongation and total elongation significantly recovered to 19.3% and 21.8%, respectively. The results clearly mean that, by making the microstructure a fully recrystallized UFG, the tensile ductility could be remarkably regained without sacrificing of the tensile strength.

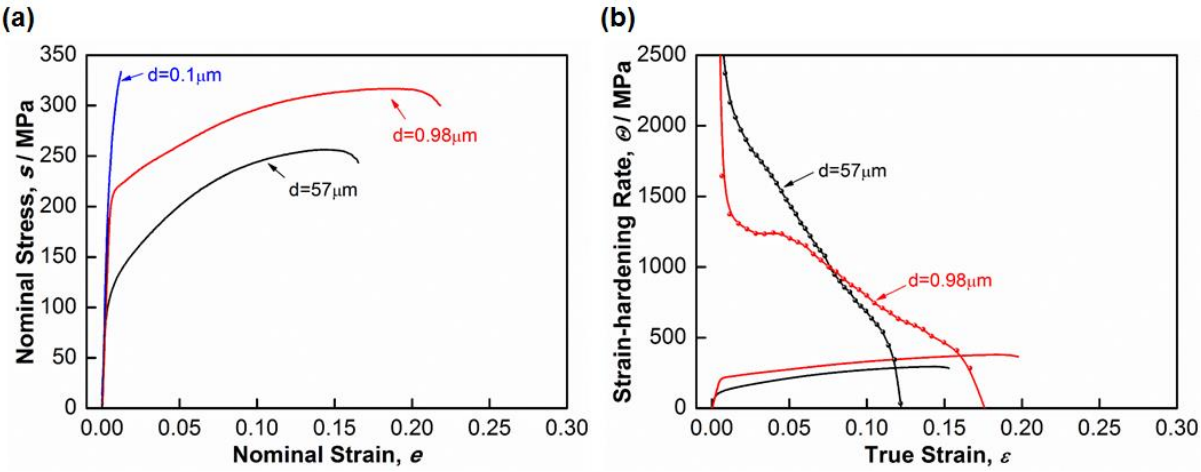


**Figure 3**. (a) Nominal stress-strain curves of the specimens having different grain sizes (*d*) after processing under different conditions. (b) The stain-hardening rate and true stress curves against the true strain of the specimens having different mean grain sizes of 0.98 μm and 57 μm.

The uniform elongation is an important parameter when considering ductility of materials. Figure 3 (b) shows strain-hardening rate and true stress against true strain of the as-ST (*d*=57μm) and UFG (*d*=0.98μm) specimens. According to the Considére criterion for plastic instability [12], the intersection between the strain-hardening rate curve and the true stress-strain curve indicates the point of plastic instability, i.e., the uniform elongation, after which necking progresses. For the as-ST specimen, the strain-hardening rate decreased quickly with the increase of the strain, resulting in an expected uniform tensile elongation of 12.4% (in nominal strain), which was not far from the experimental uniform elongation (13.9%) determined from the nominal stress-strain curve. In contrast, in the specimen having the fully recrystallized UFG structure (Fig.2: *d*=0.98μm) the drop of the strain-hardening rate was suppressed, compared with the as-ST specimen, so that the plastic instability was

delayed. The plastic instability point obtained from Fig.3 (b) (16.8% nominal strain) was again not far from the uniform elongation (19.3%) obtained from the nominal stress-strain curve (Fig.3 (a)). Consequently, it can be concluded that the large tensile ductility in the present annealed specimen is attributed to the enhanced strain-hardening ability realized in the fully recrystallized UFG structure.

In order to reveal underlying deformation mechanisms realizing the enhanced strain-hardening behavior in the fully recrystallized UFG specimen, the deformation microstructures were observed after tensile deformation to specified strains. Figure 4 shows the EBSD maps of the as-ST and the UFG specimens at a tensile strain of 10%. Colors in the IPF maps (Fig.4 (a) and (c)) indicate crystallographic orientations parallel to the normal direction of the sheet-type tensile specimens. As shown in Figure 4 (a) and (b), high density of lenticular-shaped deformation twins with an area fraction of 12.1% were generated in the as-ST specimen. Crystallographic analysis indicated that the twins were exclusively {10-12} extension twins. It is known that {10-12} extension twinning has much lower critical resolved shear stress (CRSS) compared to other twinning systems [13]. In contrast, quite limited number of deformation twins with an area fraction of only 1.1% formed in the UFG specimen at the same tensile strain.

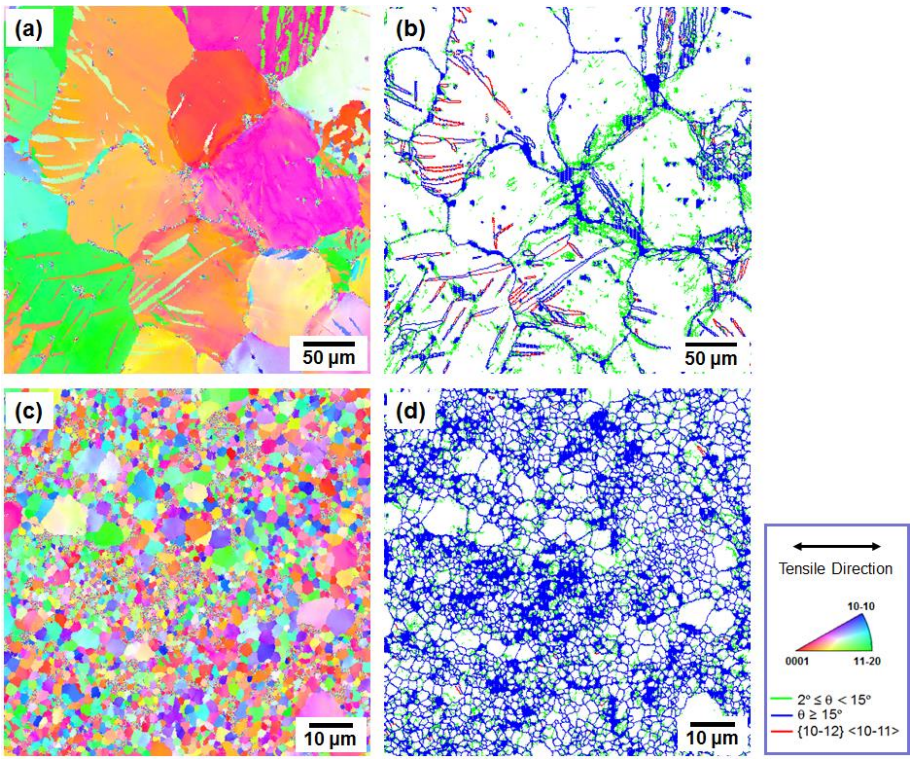


**Figure 4**. EBSD (a) IPF map and (b) corresponding GB map of the as-ST specimen ($d$=57μm) after 10% tensile deformation, showing large number of deformation twins. (c) IPF map and (d) corresponding GB map of the UFG specimen ($d$=0.98μm) after 10% tensile deformation, showing limited number of deformation twins.

Although deformation twinning was significantly inhibited in the UFG specimen, it exhibited enhanced strain-hardening and better ductility compared to the as-ST specimen. Thus, there must be some other deformation mechanisms responsible for the enhanced strain-hardening and ductility, for example, the activation of non-basal slip systems. As the major slip system, i.e., basal slip, of Mg and Mg alloys has only <***a***> component in its Burgers vector, any deformation mechanisms involving <***c***> deformation component is considered to be necessary for large plasticity [14, 15]. Koike *et al.* [14] reported a large tensile elongation up to 47% in a commercial AZ31 alloy having a mean grain size of

6.5 μm. They concluded that the superior tensile ductility was due to the activation of <***c***+***a***> non-basal slip. We are planning to make further investigations to clarify this issue in the present material.

## 4. Conclusion

In summary, a fully recrystallized UFG ZKX600 Mg alloy having a mean grain size of 0.98 μm was successfully fabricated by the combination of HPT and subsequent annealing. Simultaneously enhanced strength and ductility were realized in the UFG specimen, which were attributed to grain boundary strengthening and enough strain-hardening ability realized in the fully recrystallized UFG structure. Deformation microstructures indicated that deformation twinning was significantly inhibited in the UFG specimen. Activation of non-basal slip systems having <***c***> component was suggested in the UFG specimen, which will be confirmed in our future study.

## Acknowledgments

This work was financially supported by the Elements Strategy Initiative for Structural Materials (ESISM) and the Grant-in-Aid for Scientific Research (S) (No. 15H05767), both through the Ministry of Education, Culture, Sports, Science and Technology (MEXT), Japan.

## References

[1] Kim N 2014 *Mater. Sci. Technol.* **30** 1925.
[2] Suh B, Shim M, Shin K and Kim N 2014 *Scr. Mater.* **84** 1.
[3] Hono K, Mendis C, Sasaki T and Oh-Ishi K 2010 *Scr. Mater.* **63** 710.
[4] Agnew S and Nie J 2010 *Scr. Mater.* **63** 671.
[5] Kim W, Jeong H and Jeong H 2009 *Scr. Mater.* **61** 1040.
[6] Tsuji N, Saito Y, Lee Y and Minamino Y 2003 *Adv. Eng. Mater.* **5** 338.
[7] Kulyasova O, Islamgaliev R, Mingler B and Zehetbauer M 2009 *Mater. Sci. Eng. A* **503** 176.
[8] Zhilyaev A and Langdon T 2008 *Prog. Mater. Sci.* **53** 893.
[9] Meng F, Rosalie J, Singh A, Somekawa H and Tsuchiya K *Scr. Mater.* **78** 57.
[10] An X, Wu S, Zhang Z, Figueiredo R, Gao N and Longdon T 2012 *Scr. Mater.* **66** 227.
[11] Edalati K, Yamamoto A, Horita Z and Ishihara T 2011 *Scr. Mater.* **64** 880.
[12] Dieter G 1986 *Mechanical Metallurgy* New York, McGraw-Hill.
[13] Barnett M 2007 *Mater. Sci. Eng. A* **464** 1.
[14] Koike J, Kobayashi T, Mukai T, Watanabe H, Suzuki M, Maruyama K and Higashi K 2003 *Acta Mater.* **51** 2055.
[15] Sun J, Trimby P, Yan F, Liao X, Tao N and Wang J 2013 *Scr. Mater.* **69** 428.